

# Top Quark Forward-Backward Asymmetry and $W'$ -Boson with General Couplings

Seyed Yaser Ayazi, Sara Khatibi, and Mojtaba Mohammadi Najafabadi

*School of Particles and Accelerators,  
Institute for Research in Fundamental Sciences (IPM)  
P.O. Box 19395-5531, Tehran, Iran*

## Abstract

The measured forward-backward asymmetry in top pair events at the Fermilab Tevatron collider deviates significantly from the standard model expectation. Several models have been proposed to describe the observed asymmetry which grows with the rapidity difference of the top pairs and also with the  $t\bar{t}$  invariant mass. The presence of a heavy charged gauge boson  $W'$  with the coupling  $W' - t - d$  (left-handed, right-handed, and a mixture of left and right-handed couplings) could generate the desired top forward-backward asymmetry keeping the top pair cross section consistent with the standard model prediction. Such  $W'$ -boson makes contribution to the electric dipole moment of the neutron through contribution to the  $d$ -quark electric dipole moment, recently measured charge asymmetry ( $A_C$ ) by the LHC experiments, and the total cross section of top pair at the LHC and Tevatron. We show that the upper bounds on neutron and top electric dipole moments disfavour any  $W'$  with a mass below 240 GeV which could explain the Tevatron forward-backward asymmetry. It is shown that the charge asymmetry provides an allowed region in the parameters space with no overlap with the allowed region where the asymmetry could be described.

PACS number(s): 14.65.Ha, 12.60.-i

# 1 Introduction

Examination of the top quark interactions with other particles offer a window to possible new physics beyond the standard model (SM). Top quark with a mass close to the vacuum expectation value  $v \simeq 246$  GeV, seems to be more sensitive to the electroweak symmetry breaking mechanism than other standard model particles. At hadron colliders, top quarks are produced either singly via electroweak interactions or in pair via strong interactions with larger cross section. Many  $t\bar{t}$  events have been produced at Tevatron and LHC up to now and their experiments provide the possibility to study the top quark properties [1],[2],[3].

So far, the only observed inconsistency with the standard model predictions has been the forward-backward asymmetry in top pair production at the Tevatron. The top quark forward-backward asymmetry is defined as the difference of the number of events with  $\cos\theta > 0$  and  $\cos\theta < 0$ , where  $\theta$  is the top quark production angle in the  $t\bar{t}$  rest frame:

$$A_{FB} = \frac{N_t(\cos\theta > 0) - N_t(\cos\theta < 0)}{N_t(\cos\theta > 0) + N_t(\cos\theta < 0)} \quad (1)$$

The measured  $A_{FB}$  from the CDF and D0 experiments are  $A_{FB} = 0.158 \pm 0.075$  [4],  $A_{FB} = 0.196 \pm 0.065$  [5]. These measurements do not agree with the SM expectation, 0.089 [6],[7],[8],[9]. Since the sign of  $\cos\theta$  and  $y_t - y_{\bar{t}}$  are the same, the forward-backward asymmetry could be defined through the difference between the rapidities of top and anti-top quarks according to the following relation:

$$A_{FB} = \frac{N_t(y_t > y_{\bar{t}}) - N_t(y_t < y_{\bar{t}})}{N_t(y_t > y_{\bar{t}}) + N_t(y_t < y_{\bar{t}})} \quad (2)$$

An interesting observation is that the CDF Collaboration measured the asymmetry as a function of the invariant mass of  $t\bar{t}$  and found that the deviations of asymmetry grow with  $m_{t\bar{t}}$  [10]. While measurements of the differential cross section of  $d\sigma/dm_{t\bar{t}}$  show a good agreement with the SM expectations and therefore no evidence of beyond SM physics in  $m_{t\bar{t}}$  spectrum. Accordingly, one should note that any new physics which explains the  $t\bar{t}$  forward-backward asymmetry must satisfy all other measurements consistent with the SM predictions. There have been several models proposed to describe the observed asymmetry by Tevatron experiments [11],[12],[13],[14],[15],[16],[17],[18],[19],[20].

One of the models is proposing a new heavy charged gauge boson with the following coupling

to the top quark [21]:

$$\mathcal{L} = -g' W_\mu'^+ \bar{t} \gamma^\mu (g_L P_L + g_R P_R) d + h.c. \quad (3)$$

where  $g'$  is the coupling constant,  $g_{R,L}$  are the chiral couplings of the  $W'$  boson with fermions,  $P_{L,R} = (1 \pm \gamma_5)/2$  are the chirality projection operators. Recent LHC data excluded the existence of any SM-like  $W'$ -boson ( $g' = g, g_L = 1, g_R = 0$ ) by direct measurements into final states of leptons below the mass of 2.15 TeV [22]. Therefore, we do not consider a SM-like  $W'$ -boson in this analysis.

The new Lagrangian involving  $W'$  interactions with the top quark and  $d$ -quark leads to new diagram for top pair production at the Tevatron and LHC through the subprocess  $d\bar{d} \rightarrow t\bar{t}$ . Hence, it contributes to the differential and total cross sections of  $t\bar{t}$  at the LHC and Tevatron.

In addition to the  $t\bar{t}$  production cross section, the  $W'$ -boson introduced in the new Lagrangian in Eq.3, can induce new contribution to the  $d$ -quark electric dipole moment.

In this letter, three categories of this model according to different values of  $g_{L,R}$  are considered: (1)  $g_L = g_R = 1$  ( $g'$  and  $M_{W'}$  are free parameters). (2)  $g_L = 0, g_R = 1$  ( $g'$  and  $M_{W'}$  are free parameters). (3)  $g'$  is removed and in general  $g_L, g_R$  and  $M_{W'}$  are free parameters. Then, we try to find allowed regions in the parameters space consistent with the top pair cross section at the LHC, Tevatron, the forward-backward asymmetry, upper limits on the top and  $d$ -quark electric dipole moment, and finally the charge asymmetry in  $t\bar{t}$  events.

The paper is organized as follows. The next section is dedicated to describe the new physics corrections to the top pair production cross section. In section 3, we describe the role of new Lagrangian in the electric dipole moments of  $d$ -quark and top quark. And finally, a numerical calculations and discussion on the results are presented in section 4.

## 2 Cross Sections and Charge Asymmetry

As mentioned in the previous section, in addition to the  $s$ -channel diagram from the gluon exchange (SM contribution) in  $d\bar{d} \rightarrow t\bar{t}$  process, a  $t$ -channel diagram due to  $W'$  exchange has to be added in the calculations. Therefore, the squared matrix element ( after ignoring the  $d$ -quark mass, summing over the spin and color, and averaging over the color and spin of the initial

partons) has the following form [21],[23]:

$$\begin{aligned} |\overline{\mathcal{M}}|^2 = & \frac{4g_s^4}{9\hat{s}^2}(u_t^2 + t_t^2 + 2\hat{s}m_t^2) + \frac{4g'^2g_s^2}{9\hat{s}t_{W'}}(g_L^2 + g_R^2)[2u_t^2 + 2\hat{s}m_t^2 + \frac{m_t^2}{M_{W'}^2}(t_t^2 + \hat{s}m_t^2)] + \\ & \frac{g'^4}{4t_{W'}^2}[4((g_L^4 + g_R^4)u_t^2 + 2g_L^2g_R^2\hat{s}(\hat{s} - 2m_t^2)) + \frac{m_t^4}{M_{W'}^4}(g_L^2 + g_R^2)^2(t_t^2 + 4M_{W'}^2\hat{s})] \end{aligned} \quad (4)$$

where  $\hat{s}, t, u$  are mandelstam parameters, and  $u_t = u - m_t^2, t_t = t - m_t^2, t_{W'} = t - M_{W'}^2$ . The first term in the above amplitude is the SM contribution, the second term is the interference term between the standard model and the new diagram arising from  $W'$ -exchange, and the last term is the contribution of  $W'$ -boson exchange.

The total and differential cross sections at hadron colliders can be obtained by convoluting the partonic cross section with the parton distribution functions (PDF) for the initial hadrons. Using CTEQ6L [24] set as the parton distribution functions, the total cross section at the Tevatron and LHC is calculated. The top quark forward-backward asymmetry is also calculated according to the Eq.1.

The total measure production cross section of the  $t\bar{t}$  at the Tevatron and the LHC are [25],[26]:

$$\sigma_{\text{Tevatron}} = 7.56 \pm 0.63 \text{ pb} , \quad \sigma_{\text{LHC}} = 165 \pm 13.3 \text{ pb}. \quad (5)$$

At the LHC, since the initial state is symmetric (proton-proton), the top quark forward-backward asymmetry vanishes. However, an asymmetry in charge  $A_C$  can be measured, which is defined as the relative difference between  $t\bar{t}$  events with  $|y_t| > |y_{\bar{t}}|$  and  $|y_t| < |y_{\bar{t}}|$ . Where  $y_t(y_{\bar{t}})$  are the rapidity of the top (anti)quark in the laboratory frame. In proton-proton collisions at the LHC, the  $u, d$  valence quarks carry larger average momentum fraction than the anti-quarks. This leads to a boost of the  $t\bar{t}$  system along the direction of the *incoming quark*, and therefore to a larger average rapidity for top quarks than anti-top quarks. The ATLAS and CMS measurements for the charge asymmetry are:  $A_C = -0.018 \pm 0.036$  [27],  $A_C = -0.013 \pm 0.041$  [28], and the SM prediction is  $A_C = 0.0115$  [9]. It is notable that within the uncertainties the standard model prediction for charge asymmetry is in agreement with the measured values at the LHC. From another side, since there is some tension between the asymmetry in charge at the LHC and the forward-backward asymmetry at the Tevatron, it was expected to observe an enhancement of  $A_C$  at the LHC [29],[30].

We probe the parameters space of considered model in Eq.3 with the current measured  $t\bar{t}$

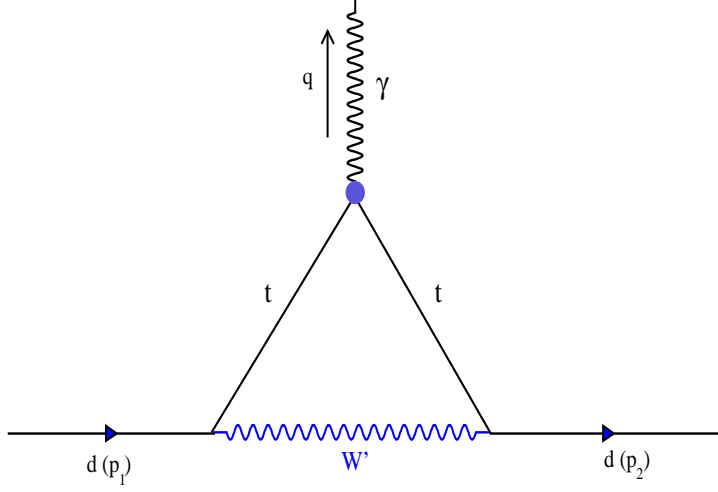


Figure 1: *Diagram contributing to the on-shell  $q\bar{q}\gamma$  vertex arising from the  $W'$  interactions.*

production cross section both at the Tevatron and the LHC, the forward-backward asymmetry, and the charge asymmetry of top pair events at the LHC.

### 3 Electric Dipole Moment Analysis

The electric dipole moment of a spin 1/2 particle is defined by the effective Lagrangian [31]:

$$\mathcal{L} = -\frac{i}{2}d_f\bar{\psi}\sigma_{\mu\nu}\gamma_5\psi F^{\mu\nu} \quad (6)$$

where  $d_f$  stands for the fermion  $f$  electric dipole moment. We notice that this Lagrangian is CP violating while the common standard model term which describes the interaction of a fermion with photon ( $-iQe\gamma_\mu$ ) is CP conserving. More information about electric dipole moment and CP violation effects can be found in several papers such as [31],[32],[33].

The contribution of the new couplings of  $W' - t - d$  to the on-shell  $q\bar{q}\gamma$  coupling is given by the diagram shown in Fig. 1. The respective one-loop vertex is:

$$\Gamma_\mu = -g^2 d_t \int \frac{d^4 k}{(2\pi)^4} \frac{g^{\alpha\beta} \gamma_\alpha (g_L P_L + g_R P_R) (\not{k} - \not{p}_2 + m_t) \gamma_5 \sigma_{\mu\nu} q^\nu (\not{k} - \not{p}_1 + m_t) \gamma_\beta (g_L P_L + g_R P_R)}{(k^2 - M_{W'}^2)((k - p_1)^2 - m_t^2)((k - p_2)^2 - m_t^2)} \quad (7)$$

where  $k$  is the momentum of the  $W'$ -boson,  $p_{1,2}$  are the momenta of the  $d$ -quark as depicted in Fig. 1. There are contributions to electric and magnetic dipole moments of the  $d$ -quark,

however, we are only interested in CP violating terms. After some algebraic manipulations, using Gordon identity and Dirac equation and finally integration over  $k$ , we obtain:

$$d_d = \frac{g'^2 d_t}{16\pi^2} [2x_d x_t (g_L^2 + g_R^2) + 16x_d^2 g_R g_L] f(x_t, x_d) \quad (8)$$

where  $x_t = m_t^2/M_{W'}^2$ ,  $x_d = m_d^2/M_{W'}^2$ , and

$$f(x_t, x_d) = \int_0^1 dx \int_0^{1-x} dy \frac{1-x-y}{1-(1-x_t)(x+y)-x_d(1-x-y)(x+y)} \quad (9)$$

In the denominator of the integrand in Eq.9, the third term is neglected because  $x_d$  is negligible with respect to  $x_t$  ( $x_d/x_t \sim 10^{-9}$ ). Furthermore, we will see that the second term of Eq.8 does not affect the results due to the same reason. The two-dimensional integral can be approximated as:

$$f(x_t) = \frac{x_t^2 - 1 - 2x_t \log x_t}{2(x_t - 1)^3} \quad (10)$$

At  $x_t = 1$  or  $M_{W'} = m_t$ , this function is indeterminate and it approaches  $\frac{1}{6}$  when  $x_t \rightarrow 1$ . However, as discussed in [21], if the  $W'$  is light enough the top quark can decay into a  $d$ -quark and a  $W'$ -boson and definitely, it would have been already observed in the top quark decays at the Tevatron. Therefore, in this work we concentrate on the  $W'$  boson with a mass higher than 200 GeV.

Now, we use one of the most used approach to predict the quark electric dipole moment contribution to the neutron electric dipole moment. This originates from the  $SU(6)$  quark model, with assuming a non-relativistic wave-function to the neutron. The neutron electric dipole moment has the following form in terms of quarks electric dipole moments [31]:

$$d_n = \eta \left( \frac{4}{3} d_d - \frac{1}{3} d_u \right) \quad (11)$$

where  $d_d, d_u$  are the down and up quark electric dipole moments, respectively. The QCD correction factor  $\eta$  is around 0.61.

The current experimental upper limit on the neutron electric dipole moment is  $d_n < 2.9 \times 10^{-26}$  e.cm. [34],[35]. Future experiments are able to measure the neutron electric dipole moment down to  $10^{-28}$  e.cm. Therefore, in addition to current limit, we also present the results with the future upper bound [36].

Applying the upper limits on the top quark and neutron electric dipole moments in Eq.8 provides consistent region in the  $(g', M_{W'})$  plane with these values.

The upper limit on top quark electric dipole moment has been extracted from the upper limit on the branching ratio of  $b \rightarrow s\gamma$ . It has been found to be less than  $10^{-16}$  e.cm. [37],[38].

## 4 Numerical Results and Discussion

In the numerical calculations, the top quark mass has been set  $m_t = 172.5$  GeV. The contributions of the new physics with  $W' - d - t$  to the observables defined in section 2 at the partonic level is calculated by employing CTEQ6L parton distribution functions [24]. The calculation is performed at fixed renormalization and factorization scale  $\mu_R = \mu_F = m_t$ . To include the effect of higher order QCD corrections to the observables, all observables are normalized to ratio of measured experimental cross section to the leading order SM cross section. The major QCD corrections within the  $W'$  model have only been computed in [23] and led to almost the same as pure SM higher order QCD corrections.

In order to obtain the relevant parameters of the  $W'$  model, we scan the region  $200 < M_{W'} < 800$  GeV in three different categories.

- $g_L = 0, g_R = 1$ : The area of  $g'$  coupling versus  $M_{W'}$  consistent with Tevatron measurement of the  $A_{FB}$  asymmetry is the band between two green curves in Fig.2. The regions between the  $M_{W'}$ -axis and the dashed lines are allowed regions which are consistent with the LHC and Tevatron top pair cross section measurements. The consistent region with the LHC measurement of charge asymmetry is the region between the red solid curve and the  $M_{W'}$ -axis. The area under the black (blue) curve is the allowed region in the  $M_{W'}, g'$  plane that arises from the electric dipole moment bound of  $10^{-26}$  ( $10^{-28}$ ) e.cm.

As it can be seen in Fig. 2, the acceptable values for  $g_R$  increases slightly with the mass of  $W'$ . The electric dipole moment excludes any right-handed  $W'$  with the mass below 240 GeV which could explain the forward-backward asymmetry. Since there is no overlapping region between the measured charge asymmetry at the LHC and  $A_{FB}$  area,  $A_C$  disfavors right-handed  $W'$ -boson which could explain the top quark forward-backward asymmetry.

Other interesting point depicted in Fig. 2 is the allowed values of  $g'$  and  $M_{W'}$  arising from

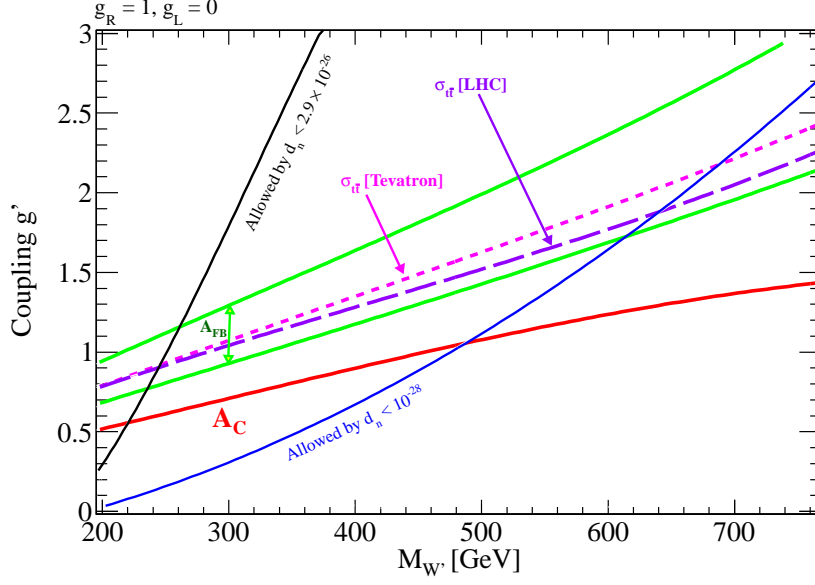


Figure 2: Region of  $W'$  coupling in terms of  $M_{W'}$  consistent with Tevatron measurements of the  $t\bar{t}$  forward-backward asymmetry (region between two green curves). The areas between the  $M_{W'}$ -axis and the dashed curves are consistent with the LHC and Tevatron cross sections. The consistent region with the LHC charge asymmetry is the area between the solid red curve and  $M_{W'}$ -axis. The area under the black curve is the allowed region coming from limits on electric dipole moments. The region under the blue curve is corresponding to the allowed region with  $10^{-28}$  as for the neutron electric dipole moment.

the future upper limit on the neutron electric dipole moment. Future experiments are able to measure the electric dipole moment of neutron down to  $10^{-28}$  e.cm., i.e. two orders of magnitude better than the present limits [36]. In Fig.2, the light blue points are the allowed region according to the future bound on the neutron electric dipole moment. As it can be seen neutron electric dipole moment would be able to exclude the existence of any right-handed  $W'$ -boson with a mass below 600 GeV which could explain the forward-backward asymmetry. As a consequence of the behaviour of  $f(x)$  in Eq.10 at  $x = 1$ , some points are allowed at  $M_{W'} = m_t$  which can be seen in Fig.2.

- $g_L = g_R = 1$ : As depicted in Fig. 3, the consistent area in the plane of  $g'$  coupling and  $M_{W'}$  with Tevatron measurement of the  $A_{FB}$  asymmetry (the band between two green curves) and the LHC and Tevatron top pair cross section measurements is small. In other words, only low



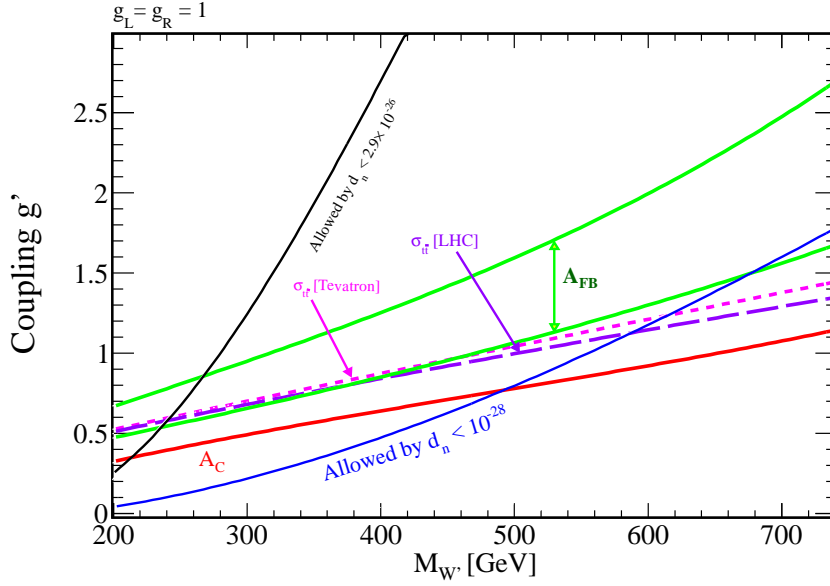


Figure 3: Region of  $W'$  coupling with  $g_L = g_R = 1$  versus  $M_{W'}$  consistent with Tevatron measurements of the  $t\bar{t}$  forward-backward asymmetry (region between two green curves). The areas between the  $M_{W'}$ -axis and the dashed curves are consistent with the LHC and Tevatron cross sections. The consistent region with the LHC charge asymmetry is the area between the solid red curve and  $M_{W'}$ -axis. The area under the black curve depicts the allowed region arises from bounds on electric dipole moments. The region under the blue curve is corresponding to the allowed region with  $10^{-28}$  e.cm as for the neutron electric dipole moment.

mass vector like  $W'$  can satisfy the values of  $A_{FB}$  and cross sections. The regions between  $M_{W'}$ -axis and the dashed lines are allowed regions consistent with the LHC and Tevatron top pair cross section measurements. Only the region of  $M_{W'}$  below 320 GeV can explain the asymmetry. While the current limit on electric dipole moment of neutron disfavors the  $W'$ -boson mass up to 240 GeV. Similar to the latter case, the charge asymmetry measurement does not have any overlapping region with the favorite region. Combining the electric dipole moment limit with the cross section limits, we find that only  $W'$  boson with  $240 < M_{W'} < 320$  GeV is consistent with the Tevatron  $A_{FB}$ .

The same as previous case, as shown in Fig. 3, the light blue dots are the allowed region according to the future bound on the neutron electric dipole moment. Clearly, the future limit on neutron electric dipole moment is able to exclude a vast region in the  $(g', M_{W'})$  plane which could explain the forward-backward asymmetry. Therefore, this case of  $W'$  coupling is not able to describe the asymmetry because of the cross sections limits.

- $g' = 1$ , arbitrary  $g_L, g_R$ : In this case, there are three parameters  $g_L, g_R$  and  $M_{W'}$  which could be found in such a way that the top forward-backward asymmetry be generated. Figs.4 show the regions consistent with the measured top pair cross sections at the Tevatron (depicted by plus symbol), LHC (empty squares), and the Tevatron  $t\bar{t}$  forward-backward asymmetry (empty circles) for  $M_{W'} = 300$  (left top), 500 (right top), 700 GeV (bottom). We note that the electric dipole moment bounds do not provide comparable results with the other measurements. Comparison of plots for  $M_{W'} = 300$  GeV and  $M_{W'} = 500, 700$  GeV leads to the fact that the overlapping region between the measured cross sections and the Tevatron forward-backward asymmetry gets smaller with increasing the  $W'$ -boson mass. According to Figs. 4, with growing the  $W'$ -boson mass the cross sections and forward-backward asymmetry are both satisfied by either large  $g_L$  or large  $g_R$ . It means that in the  $(g_L, g_R)$  plane, the regions with intermediate values of  $g_R$  and  $g_L$  are excluded. It also could be seen in Fig. 3, with increasing  $M_{W'}$  the overlapping area decreases because of different slopes of cross sections and  $A_{FB}$  lower limit curve. However, in analogy with the previous cases, no overlapping region between the LHC charge asymmetry (pink squares) and the Tevatron top forward-backward asymmetry is seen.

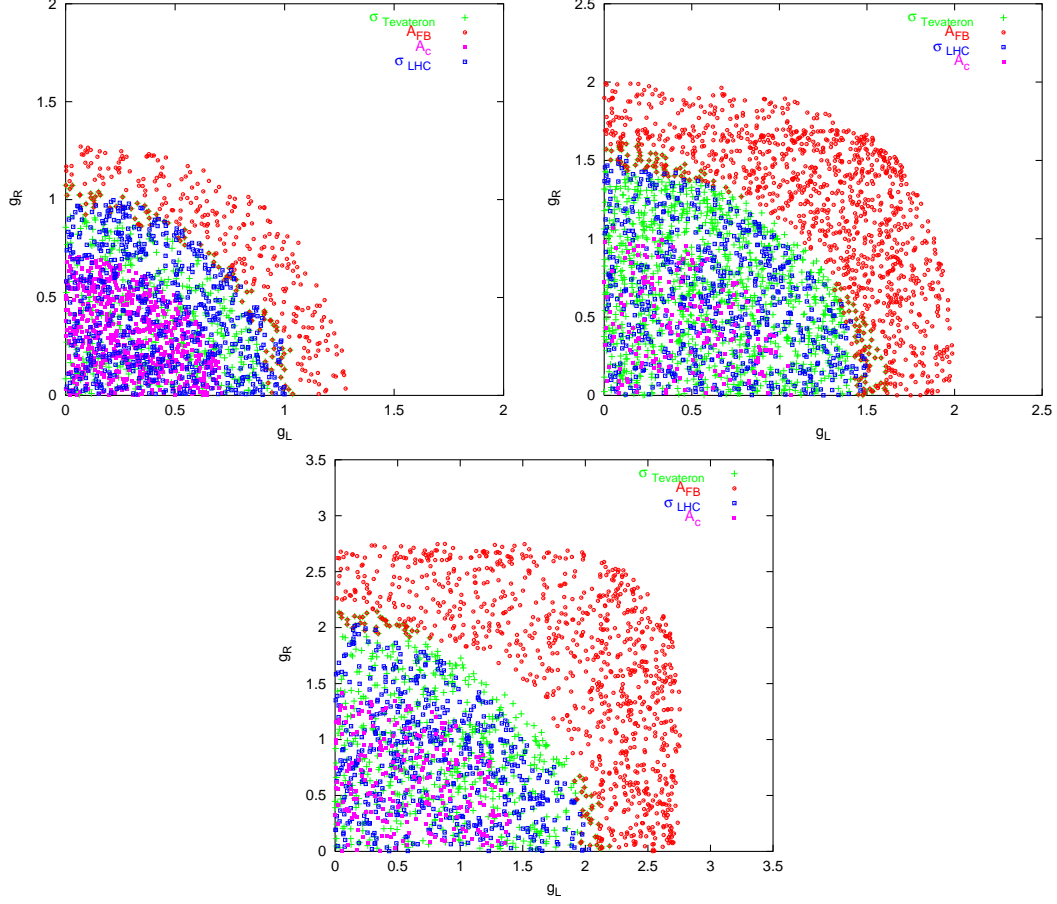


Figure 4: The allowed regions consistent with the Tevatron forward-backward asymmetry,  $t\bar{t}$  cross sections at the LHC and Tevatron, the LHC charge asymmetry with general values of  $g_R, g_L$  couplings. In the left top plot  $M_{W'} = 300$  GeV and for the right top plot  $M_{W'}$  is equal 500 GeV, in the bottom plot  $M_{W'} = 700$  GeV.

## 5 Conclusions

In this paper, we investigated the consistency of heavy charged vector boson  $W'$  with the existing  $t\bar{t}$  production measurements. Various cases of  $W'$  couplings with top and down quarks are examined: right-handed  $W'$  ( $g_L = 0, g_R = 1$ ), vector-like ( $g_L = g_R = 1$ ), and in general mixture of left and right-handed (arbitrary  $g_{L,R}$ ). We find no overlapping region between the large positive  $t\bar{t}$  forward-backward asymmetry measurements at the Tevatron and the LHC charge asymmetry measurements in all cases. Apart from the LHC charge asymmetry, the electric dipole moment limits do not support a  $W'$  boson below 240 GeV which could explain the Tevatron forward-backward asymmetry. We also found that the future upper limit on the neutron electric dipole moment is not in favor of any right-handed  $W'$ -boson with a mass under around 600 GeV which could explain the top quark forward-backward asymmetry.

• **Note added** At around the same time as our paper was being written a related analysis of the charge asymmetry part with right-handed coupling  $W'$  appeared in [39].

## References

- [1] W. Bernreuther, arXiv:0805.1333 [hep-ph].
- [2] M. Beneke *et al.*, arXiv:hep-ph/0003033.
- [3] W. Bernreuther, P. Gonzalez and M. Wiebusch, Eur. Phys. J. C **60** 197 (2009), arXiv:0812.1643 [hep-ph].
- [4] T. Aaltonen *et al.* [CDF Collaboration], Phys. Rev. D 83, 112003 (2011).
- [5] V. Abazov *et al.* [D0 Collaboration], Phys. Rev. Lett. 84, 112005 (2011), arXiv:1107.4995 [hep-ex].
- [6] P. Ferrario and G. Rodrigo, Phys. Rev. D 78, 094018 (2008).
- [7] W. Bernreuther and Z. G. Si, Nucl. Phys. B 837, 90 (2010).
- [8] W. Hollik and D. Pagani, arXiv:1107.2606 [hep-ph].
- [9] J. H. Kuhn and G. Rodrigo, JHEP 1201, 063 (2012).

- [10] The CDF Collaboration, CDF Note 10807.
- [11] P. Ferrario and G. Rodrigo, Phys. Rev. D 80, 051701 (2009) [arXiv:0906.5541 [hep-ph]].
- [12] J. A. Aguilar-Saavedra and M. Perez-Victoria, Phys. Lett. B 705, 228 (2011) [arXiv:1107.2120 [hep-ph]]; G. M. Tavares and M. Schmaltz, Phys. Rev. D 84, 054008 (2011) [arXiv:1107.0978 [hep-ph]].
- [13] S. Jung, H. Murayama, A. Pierce and J. D. Wells, Phys. Rev. D 81, 015004 (2010) [arXiv:0907.4112 [hep-ph]].
- [14] K. Blum, Y. Hochberg and Y. Nir, JHEP 1110, 124 (2011) [arXiv:1107.4350 [hep-ph]].
- [15] J. Shu, T. M. P. Tait and K. Wang, Phys. Rev. D 81, 034012 (2010) [arXiv:0911.3237 [hep-ph]].
- [16] R. Barcelo, A. Carmona, M. Chala, M. Masip and J. Santiago, arXiv:1110.5914 [hep-ph].
- [17] R. Barcelo, A. Carmona, M. Masip and J. Santiago, arXiv:1106.4054 [hep-ph].
- [18] R. Barcelo, A. Carmona, M. Masip and J. Santiago, Phys. Rev. D **84** (2011) 014024 [arXiv:1105.3333 [hep-ph]].
- [19] B. Bhattacharjee, S. S. Biswal and D. Ghosh, Phys. Rev. D **83**, 091501 (2011) [arXiv:1102.0545 [hep-ph]].
- [20] B. Grinstein, C. W. Murphy, D. Pirtskhalava and P. Uttayarat, arXiv:1203.2183 [hep-ph].
- [21] K. Cheung, W. -Y. Keung and T. -C. Yuan, Phys. Lett. B **682**, 287 (2009) [arXiv:0908.2589 [hep-ph]].
- [22] G. Aad et al. (ATLAS Collaboration), Phys. Lett. B 705, 28 (2011).
- [23] K. Yan, J. Wang, D. Y. Shao and C. S. Li, Phys. Rev. D **85**, 034020 (2012) [arXiv:1110.6684 [hep-ph]].
- [24] J. Pumplin, D. R. Stump, J. Huston, H. L. Lai, P. M. Nadolsky and W. K. Tung, JHEP **0207**, 012 (2002) [arXiv:hep-ph/0201195].
- [25] D0 Collaboration, Phys. Lett. B 704, (2011) 403-410.

- [26] The CMS Collaboration, CMS-PAS-TOP-11-024.
- [27] G. Aad et al. [ATLAS Collaboration], arXiv:1203.4211 [hep-ex].
- [28] S. Chatrchyan *et al.* [CMS Collaboration], Phys. Lett. B **709**, 28 (2012) [arXiv:1112.5100 [hep-ex]]; The CMS Collaboration, CMS PAS TOP-11-030.
- [29] J. A. Aguilar Saavedra and M. Perez-Victoria, Phys. Rev. D **84**, (2011) 115013.
- [30] J. A. Aguilar Saavedra and A. Juste, arXiv:1205.1898.
- [31] M. Pospelov and A. Ritz, Annals Phys. **318**, 119 (2005) [hep-ph/0504231].
- [32] T. Fukuyama, arXiv:1201.4252 [hep-ph].
- [33] A. Czarnecki and B. Krause, Phys. Rev. Lett. **78**, 4339 (1997) [hep-ph/9704355].
- [34] I. S. Altarev et al., Phys. Lett. B276, 242 (1992).
- [35] I. S. Altarev et al., Phys. Atomic Nucl. 59, 1152 (1996).
- [36] The nEDM Experiment (M. D. Cooper and S. K. Lamoreaux spokespersons), <http://p25ext.lanl.gov/edm/edm.html>.
- [37] J. L. Hewett and T. G. Rizzo, Phys. Rev. D **49**, 319 (1994) [hep-ph/9305223].
- [38] J. F. Kamenik, M. Papucci and A. Weiler, Phys. Rev. D **85**, 071501 (2012) [arXiv:1107.3143 [hep-ph]].
- [39] S. Fajfer, J. F. Kamenik and B. Melic, arXiv:1205.0264 [hep-ph].